

# CLIPS Proceedings

Sebastian Tilch\* and Rainer Mautz\*

\* Institute of Geodesy and Photogrammetry, ETH Zurich, Switzerland.  
Email: tilchs@ethz.ch

**Abstract**—This paper presents the latest developments related to an optical indoor positioning system named CLIPS. Focus is on new findings regarding the detection of laser spots in images and their unique identification. In addition a novel method of system scale determination is presented.

**Keywords** — Optical Indoor Positioning; Camera-based positioning, Camera Pose; Relative Orientation; CLIPS

## I. INTRODUCTION

The use of indoor positioning systems becomes more and more eminent in daily life. There is an increasing demand on positioning capabilities in applications such as healthcare, disaster management, metrology, logistics or housekeeping. A growing market in indoor positioning technologies appoints the research community as well as companies to satisfy this increasing demand. The successful launch of the IPIN (Indoor Positioning and Navigation) Conference in 2010 with its unprecedented number of presentations dedicated to indoor positioning techniques confirms this trend.

In addition to popular indoor positioning techniques such as those exploiting UWB- (Ultra-WideBand), WLAN- (Wireless Local Area Network) and ultrasound-signals, the alternative technique of optical indoor positioning can be found in areas of pedestrian navigation [2], [10], [11], [16], metrology [1], [4] and robot controlling [3], [4].

This paper describes an optical indoor positioning system called CLIPS (Camera and Laser-based Indoor Positioning System) and the progress that has been made subsequent to our last report [15]. It is organized in three sections. The first section briefly repeats the basic concept of CLIPS. In the second section, the new research activities related to CLIPS are detailed. The third section is dedicated to a brief outlook and a conclusion.

## II. BASIC CONCEPT

The basic concept of CLIPS is illustrated in Figure 1. In contrast to the photogrammetric relative camera orientation CLIPS is based on the principle of an inverse camera, where one camera is substituted for a device that emits laser-beams from a virtual central point. The laser beams project bright spots on any surface in an indoor environment. Thereby, the laser device represents an inverse camera. When laser spots have been captured by a mobile camera, the relative orientation of the camera to the laser-device is determined by exploiting the concepts of stereo photogrammetry. As a major advantage no high-precision mechanics or sophisticated set-ups are required,

This work is funded by the Swiss National Fund (SNF).

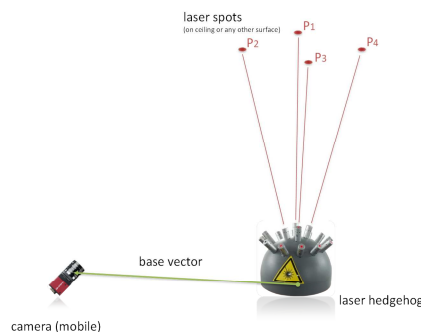


Figure 1. The camera pose, with respect to the laser hedgehog, can be estimated by capturing the projected pattern of the red laser spots.

making it a low-cost and easy-to-use system for high precision positioning.

## III. CURRENT RESEARCH ACTIVITIES

### A. Point Detection

In a first step, the laser points need to be detected in the images. For this purpose a simple intensity threshold was applied, accepting that there is no adaption to varying illumination conditions from additional light sources or varying viewing angles

In order to solve the problem of disturbing light sources, we assumed that the saturation of natural and artificial light sources in the red and green channel is almost the same. Therefore, these unwanted light sources could be eliminated by taking the difference of both colour channels and applying an intensity threshold on the difference image. Furthermore, we choose a lower sensor exposure time to reduce the influence of ambient light. As a consequence, the laser spots can be easily detected with low computational cost.

### B. Point Identification

In a second step, the detected laser spots have to be assigned to the corresponding laser beams of the hedgehog. This is a crucial task since the relative orientation algorithm requires at least five pairs of corresponding points to solve the coplanarity constraint.

The projected spot pattern consists of sixteen laser spots arranged on two concentric rings with four spots on the inner ring and twelve spots on the outer ring, as illustrated in Figure 2. The resulting symmetry can be dissolved by an additional green laser spot that is also used to solve the problem of scale determination. For the purpose of point identification it is assumed that the inner four spots and at least four laser spots of the outer ring are visible in the image. Additionally, the detected spots of the outer ring must form a convex hull around the

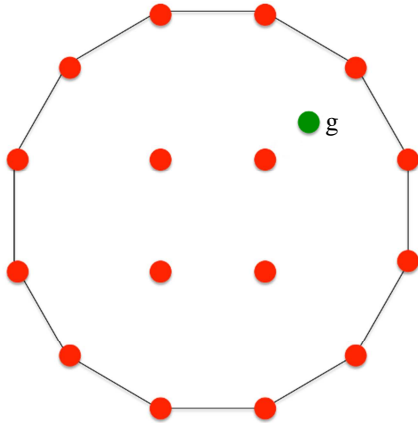


Figure 2. The projected laser spots pattern consists of two concentric rings and an additional green laser spot (marked with a 'g') for scale introduction.

inner four spots. Under these assumptions, the following steps can be applied to uniquely identify all visible laser spots.

First, the algorithm identifies points on the outer ring. This means, that the algorithm determines all spots that belong to a convex hull. All spots on this hull are assigned to the outer hull and as a consequence, all points not being part of this hull can be regarded as inner points.

Second, the inner points are identified. For that purpose, the algorithm makes use of an additional green laser spot as shown in Figure 2. The four inner points with the smallest distances to the green laser spot belong to the inner ring. One of these four spots is closest to the green spot compared to the other three spots. This laser spot is denoted with ID 3. The remaining three points are labeled clockwise with IDs 2, 1 and 4. Now, all spots on the inner ring are identified.

Third, the laser spots on the outer ring are identified. For this purpose, every spot of the outer ring is assigned to one of the six possible lines between the four spots of the inner circle. In Figure 3, two of these six lines are shown. According to Tilch [14], the distances between each spot  $x_i$  on the outer circle and each line  $g$  (that is defined by the vector  $\mathbf{r}$  and an initial point  $\mathbf{x}_{IP}$ ) can be calculated by

$$d_i = \|(\mathbf{E} - \mathbf{nn}^T)(\mathbf{x}_i - \mathbf{x}_{IP})\|, \quad (1)$$

where

$$\mathbf{n} = \frac{\mathbf{r}}{\|\mathbf{r}\|}. \quad (2)$$

In our case, the initial point  $\mathbf{x}_{IP}$  is equal to a spot of the inner circle and the vector  $\mathbf{r}$  parallel to the direction of the line. Matrix  $\mathbf{E}$  in Equation 1 denotes a 2-by-2 identity matrix and vector  $\mathbf{n}$  is the normalized vector of a line. All distances can be composed in the distance matrix  $\mathbf{D}$ ,

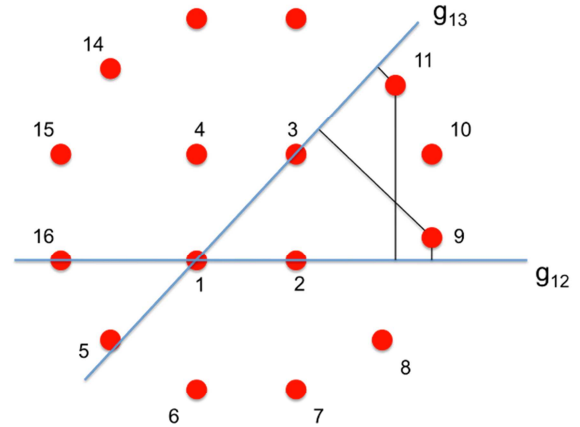


Figure 3. The fine identification queries the membership of a spot to a certain line defined by two of the four inner spots. This approach is based on a simple distance analysis.

where each row contains the distances of all spots to one line and each column contains the distances of a spot to all lines. Now, in each column the minimum distance of a spot to its nearest line is found. This way, two points of the outer ring can be associated with each of these six lines. In order to solve this ambiguity, the lines are split at the center into two rays (half lines). Which spot belongs to one of these two rays can be determined easily. Finally, all visible spots are labeled with their ID.

The benefits of this approach are twofold. Firstly, the real-time identification of all laser spots can be achieved from a single image. Secondly, just a fraction of the laser spots must be visible for their identification. The only constraint is that at least four spots on the outer ring are visible in the image and that they form a convex hull that fully encloses the inner ring.

### C. Camera Pose Estimation

The camera pose can be estimated by solving the coplanarity constraint. This constraint describes the geometrical relationship between two convergent images, where the projection centres of the images and an object point define a so called epipolar plane, see Figure 5.

Now, the task of solving the coplanarity constraint is a nonlinear problem and therefore requires good approximate values for the Relative Orientation (RO) parameters. These initial parameters are improved by an iterative least-squares adjustment. This approach requires an answer of how approximate values can be obtained.

One way is the exact algebraic solution of a set of polynomials that follow from the coplanarity constraints. Either the Gauss-Jordan elimination [12] or Gröbner bases [5], [9], [13] can be used to estimate the roots of the polynomials. Unfortunately, the solutions are not unique. An RANSAC [7] framework can be used to determine the correct solution. A possible implementation of Stewénius' 5-Point solver [13] for the CLIPS project was presented at the ISPRS Midterm Symposium in 2010 [15].

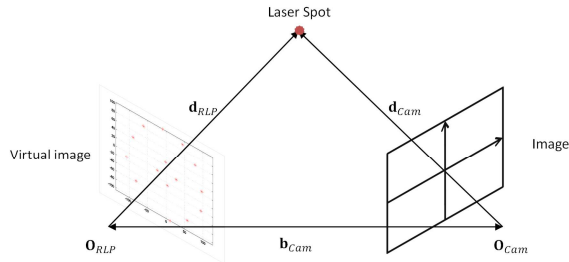


Figure 5. Epipolar Geometry

Another way of approximate value generation was proposed by Cronk et al. [8]. Hereby, the location of a second camera is simulated on a tessellated sphere around the first camera station. Starting from arbitrary initial values of the orientation angles (usually chosen to be zero) every set of initial values is improved by a least squares adjustment. The right solution can be found by considering the RMSE and the fact that the objects are always located in front of both camera stations.

In order to spare the need for a RANSAC embedment which causes high computational costs we have chosen the approach by Cronk et al. Under the assumption that the camera pose of two consecutive stations only slightly changes we can use the refined RO parameters of the previous image as initial values for the RO determination of the next image.

#### D. Introduction of the System Scale

A common approach of scale introduction is the scale estimation by extracting reference information in the image. For this purpose, we have added green laser pointers in an eccentric position to the laser hedgehog. Subsequent to the estimation of the relative orientation parameters, the system scale can be determined as shown in Figure 4. Since the direction  $\mathbf{d}_{GLP}$  of the additional laser pointer and its base line  $\mathbf{b}_{GLP}$  to the laser rig are known from a one-time calibration, the system scale can be estimated as follows. Please note that all vectors in Figure 4 are unit vectors. The factor  $b$  denotes the baseline's length between the laser-device and the additional green laser pointer.

The scale formula can be derived from the intersection of the plane  $\Pi$  spanned by the vectors  $\mathbf{d}_{GLP}$  and  $\mathbf{d}_{Cam}$  with the straight line  $l$  defined by the base vector  $\mathbf{b}_{GLP}$ . The plane

$$\Pi: (\mathbf{d}_{GLP} \times \mathbf{d}_{Cam})\mathbf{x} - b \cdot (\mathbf{d}_{GLP} \times \mathbf{d}_{Cam})\mathbf{b}_{GLP} = 0 \quad (3)$$

can be expressed by the Hessian normal form where the cross product  $(\mathbf{d}_{GLP} \times \mathbf{d}_{Cam})$  represents the normal vector and the base vector  $\mathbf{b}_{GLP}$  an initial point of that plane. The straight line

$$l: s \cdot \mathbf{b}_{Cam} - \mathbf{x} = 0 \quad (4)$$

is defined by the direction of vector  $\mathbf{b}_{Cam}$  and the hedgehog projection centre as one point.

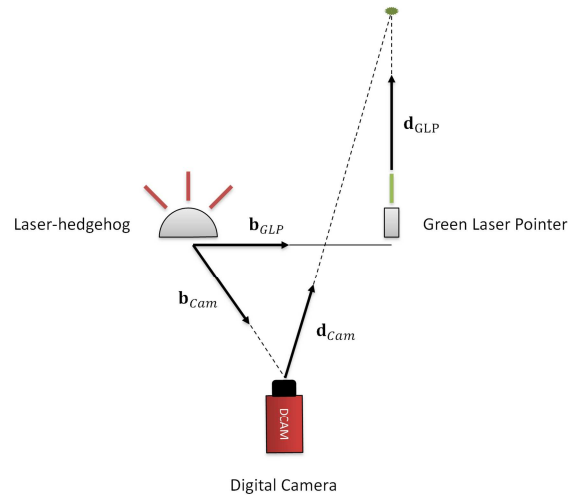


Figure 4. Introduction of the system scale

Solving (4) to vector  $\mathbf{x}$  and inserting the result in (3) leads to

$$s \cdot (\mathbf{d}_{GLP} \times \mathbf{d}_{Cam})\mathbf{b}_{Cam} - b \cdot (\mathbf{d}_{GLP} \times \mathbf{d}_{Cam})\mathbf{b}_{GLP} = 0 \quad (5)$$

and after solving for  $s$  we obtain

$$s = b \cdot \frac{(\mathbf{d}_{GLP} \times \mathbf{d}_{Cam})\mathbf{b}_{GLP}}{(\mathbf{d}_{GLP} \times \mathbf{d}_{Cam})\mathbf{b}_{Cam}} \quad (6)$$

The system scale can be introduced by scaling the vector  $\mathbf{b}_{Cam}$  with the factor  $s$ .

#### Geometrically Unstable Cases

First tests have shown that this concept reveals a geometrically unstable constellation (see Figure 6). If the base vector  $\mathbf{b}_{Cam}$  is collinear to the base vector  $\mathbf{b}_{GLP}$  then the plane  $\Pi$  contains the straight-line  $l$ . As a consequence, line  $l$  and plane  $\Pi$  do not intersect and therefore, the scale determination is ill-posed.

In order to avoid such a geometric constellation, a special hedgehog mount was constructed allowing us to point 36 green lasers in four main directions as shown in Figure 7. This means, that the scale can be estimated independently 36 times. In the worst-case scenario, reliable scale estimation can be carried out from at least two of the four main directions.

#### Scale Quality Measure

In order to determine bad scales, a scale quality measure

$$SQM = \frac{\|(\mathbf{b}_{GLP} \times \mathbf{d}_{GLP}) \times (\mathbf{b}_{Cam} \times \mathbf{d}_{GLP})\|}{\|\mathbf{b}_{GLP} \times \mathbf{d}_{GLP}\| \cdot \|\mathbf{b}_{Cam} \times \mathbf{d}_{GLP}\|} \quad (7)$$

is derived.  $SQM$  is a measure for the angle of incidence of the two planes defined by the vectors  $\mathbf{b}_{Cam}$ ,  $\mathbf{b}_{GLP}$  and  $\mathbf{d}_{GLP}$ . If these two planes become parallel then  $SQM$  approaches

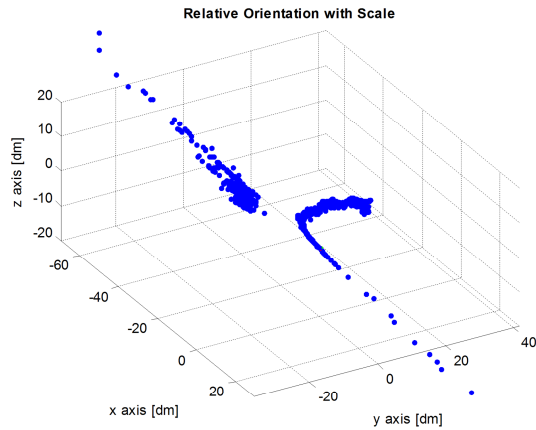


Figure 6. The track of the mobile camera reveals the asymptotic behaviour at the geometric unstable constellation



Figure 7. Laser-Hedgehog with four major axes for scale introduction

zero since the cross product of almost two collinear vectors decreases to zero. In our case the rejection criterion was chosen to be a threshold of  $SQM = 0.3827$ . If the  $SQM$  is smaller than this threshold then the scale is rejected and set to value 1. In other words, good scales can be estimated if the intersection angle of these two planes is greater than 22.5 degree.

#### IV. CONCLUSIONS AND OUTLOOK

In contrast to the previous version, the new update of the CLIPS architecture enables for the first time real-time positioning and navigation, since the laser spot identification and the introduction of the system scale can be solved image by image. Furthermore, there is no need to capture the whole pattern for a unique identification of the projected laser spots anymore. These measures have been an essential leap forward towards building a practicable system.

The next step will be to use all four major axes for scale introduction to avoid geometrical unstable cases. This step should lead to precise investigation device.

#### REFERENCES

[1] AICON 3D Systems (2010): <http://www.aicon.de>, last accessed December 2010.  
 [2] Aufderheide, D., & Krybus, W. (2010): Towards real-time camera egomotion estimation and three-dimensional scene acquisition from monocular image streams, (S. 1-10).

[3] Boochs, F., Schutze, R., Simon, C., Marzani, F., Wirth, H., & Meier, J. (2010): Increasing the accuracy of untaught robot positions by means of a multi-camera system, (S. 1-9).  
 [4] Breuckmann naviSCAN 3D. (2011): <http://www.breuckmann.com/industrie-technik/produkte/naviscan.htm>, last accessed March 2011.  
 [5] Buchberger, B. (2001): Gröbner Bases: A Short Introduction for Theorists, [http://www.risc.jku.at/publications/download/risc\\_323/2001-02-19-A.pdf](http://www.risc.jku.at/publications/download/risc_323/2001-02-19-A.pdf), [http://www.risc.uni-linz.ac.at/publications/download/risc\\_323/2001-02-19-A.pdf](http://www.risc.uni-linz.ac.at/publications/download/risc_323/2001-02-19-A.pdf). last accessed March 2011.  
 [6] Creafom Products. (2011): <http://www.creaform3d.com/en/default.aspx>, last accessed March 2011.  
 [7] Fischler, M. A., & Bolles, R. C. (1981): Random sample consensus: a paradigm for model fitting with applications to image analysis and automated cartography. *Commun. ACM*, 24, 381-395.  
 [8] Cronk, S., Fraser, C., Hanley, H.. (2006): Automated metric calibration of colour digital cameras. *The Photogrammetric Record*, 21, 355-372.  
 [9] Kalantari, M., Jung, F., Guedon, J.-P., & Paparoditis, N. (2009): The Five Points Pose Problem: A New and Accurate Solution Adapted to Any Geometric Configuration. In T. Wada, F. Huang, & S. Lin (Hrsg.), *Advances in Image and Video Technology* (Bd. 5414, S. 215-226). Springer Berlin / Heidelberg.  
 [10] Klopschitz, M., Schall, G., Schmalstieg, D., & Reitmayr, G. (2010): Visual tracking for Augmented Reality., (S. 1-4).  
 [11] Mulloni, A., Wagner, D., Barakonyi, I., & Schmalstieg, D. (2009): Indoor Positioning and Navigation with Camera Phones. *Pervasive Computing, IEEE*, 8(2), 22-31.  
 [12] Nister, D. (2004): "An efficient solution to the five-point relative pose problem," *Pattern Analysis and Machine Intelligence, IEEE Transactions on*, vol.26, no.6, pp.756-770  
 [13] Stewénius, H., Engels, C., Nistér, D. (2006): Recent developments on direct relative orientation, *ISPRS Journal of Photogrammetry and Remote Sensing, ISPRS*, vol. 60, 284-294  
 [14] Tilch, S. (2009): Calibration of CLIPS (German). Student Project Work, ETH Zurich, unpublished.  
 [15] Tilch, S., Mautz, R. (2010): Development of a new laser-based, optical indoor positioning system, *ISPRS Com. V Mid-Term Symposium*, no. 98, pp. 575-580.  
 [16] Willert, V. (2010): Optical Indoor Positioning using a camera phone, Abstract Volume, IPIN 2010, pp. 289-290